PHYSICAL REVIEW D **86,** 094010 (2012)

Transverse momentum imbalance of back-to-back particle production in $p + A$ and $e + A$ collisions

Hongxi Xing,[1,*] Zhong-Bo Kang,[2,†] Ivan Vitev,[2,‡] and Enke Wang[1,§]

[1]*Institute of Particle Physics, Central China Normal University, Wuhan 430079, China*
[2]*Theoretical Division, Los Alamos National Laboratory, Los Alamos, New Mexico 87545, USA*

(Received 19 June 2012; published 5 November 2012)

We study the nuclear enhancement of the transverse momentum imbalance for back-to-back particle production in both $p + A$ and $e + A$ collisions. Specifically, we present results for photon + jet and photon + hadron production in $p + A$ collisions, di-jet and di-hadron production in $e + A$ collisions, and heavy-quark and heavy-meson pair production in both $p + A$ and $e + A$ collisions. We evaluate the effect of both initial-state and final-state multiple scattering, which determine the strength of the nuclear-induced transverse momentum imbalance in these processes. We give theoretical predictions for the experimentally relevant kinematic regions in $d + Au$ collisions at Relativistic Heavy Ion Collider, $p + Pb$ collisions at Large Hadron Collider and $e + A$ collisions at the future Electron Ion Collider and Large Hadron Electron Collider.

DOI: 10.1103/PhysRevD.86.094010 PACS numbers: 12.38.Bx, 12.39.St, 24.85.+p, 25.75.Bh

I. INTRODUCTION

Ultrarelativistic nucleus-nucleus ($A + A$) collisions at the Relativistic Heavy Ion Collider (RHIC) and the Large Hadron Collider (LHC) have paved the way to studying important properties of a new state of matter created in such collisions, the quark-gluon plasma (QGP) [1]. In $A + A$ reactions both final-state QGP effects and initial-state cold nuclear matter effects modify experimental observables relative to the naive binary collision-scaled proton-proton ($p + p$) baseline expectation. To disentangle these effects has become a top priority for the heavy ion program. Proton-nucleus ($p + A$) collisions and electron-nucleus ($e + A$) reactions are, at present, the only tools that provide an opportunity to probe experimentally and understand theoretically cold nuclear matter effects without the complication of final-state interactions in the QGP [2–4].

Transverse momentum broadening in $p + A$ and $e + A$ collisions is among the most studied cold nuclear matter effects. When a fast parton propagates through nuclear matter, it can accumulate additional transverse momentum via multiple scattering with the soft partons inside the big nucleus either before or after the hard collision. This phenomenon is known as transverse momentum broadening, and it can be probed experimentally through the nuclear modification of single inclusive jet or hadron production in $e + A$ collisions [5–7], the nuclear broadening of Drell-Yan di-lepton or $W^{\pm}/Z^0$ boson production in $p + A$ collisions [8,9] and the Cronin effect [10,11]. One can also study the multiple scattering effects through two-particle correlations. For example, the nuclear enhancement of the transverse momentum imbalance of di-jet and di-hadron production was shown to be sensitive to both initial-state and final-state multiple scattering [12].

Different theoretical approaches have been employed to compute and describe the nuclear broadening effect. These include the dipole approach [13,14], the random walk approach [15], the diagrammatic Glauber multiple scattering [16], the color glass condensate approach [17,18], soft collinear effective theory [19–21], and the high-twist power expansion approach [5,9,12,22]. Some possible connections and relations among different frameworks have been discussed in Ref. [23]. Following our previous study [12], we will evaluate the nuclear broadening in the formalism that represents multiple scattering as contributions to the cross section from higher twist matrix elements in the nuclear state. This framework follows a well-established QCD factorization formalism for particle production in $p + A$ collisions [22,24–26], and has been previously used to describe cold nuclear matter effects, such as energy loss [27–29], dynamical shadowing [30–32] and broadening effects [5,9,12,22]. The purpose of our paper is to apply the techniques developed in our previous study of di-jet and di-hadron transverse momentum imbalance [12] to new channels, which will be accessible to the experiments in the near future. It differs from more generic parton broadening phenomenology in that the color and kinematic structures of the hard part are evaluated exactly. In particular, we will study the nuclear enhancement of the transverse momentum imbalance for photon + jet (photon + hadron) in $p + A$, di-jet (di-hadron) in $e + A$, and heavy-quark (heavy-meson) pair production in both $p + A$ and $e + A$ collisions. These two-particle correlation observables can be studied in $d + Au$ collisions at $\sqrt{s} = 200$ GeV at RHIC, the forthcoming $p + Pb$ run at $\sqrt{s} = 5$ TeV at the LHC, and at the planned Electron Ion Collider (EIC) and Large Hadron Electron Collider (LHeC). Our paper presents a unified formalism to predict theoretically this observable for multiple final-state channels.

*xinghx@iopp.ccnu.edu.cn
†zkang@lanl.gov
‡ivitev@lanl.gov
§wangek@iopp.ccnu.edu.cn

The rest of our manuscript is organized as follows: in Sec. II we study photon + jet (photon + hadron) and heavy-quark (heavy-meson) pair production in $p + A$ collisions. The beginning of this section is used to introduce the basic definition of the transverse momentum imbalance, which is common to all studied processes. We then take into account both initial-state and final-state multiple scattering to compute the nuclear enhancement in the transverse momentum imbalance of the produced back-to-back particle pair. In Sec. III we study the nuclear broadening of the transverse momentum imbalance for di-jet (di-hadron), and heavy-quark (heavy-meson) pair production in $e + A$ collisions. In Sec. IV we present our numerical estimate on the nuclear broadening for the relevant kinematics at RHIC, LHC and the future EIC and LHeC. We summarize our results in Sec. V.

II. NUCLEAR ENHANCEMENT OF THE TRANSVERSE MOMENTUM IMBALANCE IN $p + A$ COLLISIONS

The main purpose of this paper is to study the nuclear enhancement of the transverse momentum imbalance for back-to-back particle production in both $p + A$ and $e + A$ collisions, $h(P') + A(P) \to h_1(p_1) + h_2(p_2) + X$. Here h and A are the incoming hadron (or virtual photon) and the nucleus, respectively. h_1 and h_2 are the produced particles in the final state with transverse momenta $\vec{p}_{1\perp}$ and $\vec{p}_{2\perp}$. To lowest order in perturbative QCD, the production of these two particles arises from hard $2 \to 2$ scattering processes. If we denote by z the h and A collision axis, h_1 and h_2 are produced approximately back-to-back in the transverse (x, y) plane: $\vec{p}_{1\perp} \approx -\vec{p}_{2\perp}$. In $p + A$ collisions, however, the incoming parton can undergo multiple scattering before the hard collisions. The produced final-state particles are also likely to undergo multiple interactions in the big nucleus if they are strongly interacting. Both initial-state and final-state multiple scattering lead to acoplanarity, or momentum imbalance of the observed two particles. To quantify this effect, we define the transverse momentum imbalance $\vec{q}_\perp$ as

$$\vec{q}_\perp = \vec{p}_{1\perp} + \vec{p}_{2\perp}, \tag{1}$$

and the average transverse momentum squared imbalance

$$\langle q_\perp^2 \rangle = \left(\int d^2\vec{q}_\perp q_\perp^2 \frac{d\sigma}{d\mathcal{PS} d^2\vec{q}_\perp} \right) \Big/ \frac{d\sigma}{d\mathcal{PS}}. \tag{2}$$

Here, $d\sigma/d\mathcal{PS}$ is the differential cross section with $d\mathcal{PS}$ representing the relevant phase space, to be defined for each process in the corresponding section. For example, in $p + A$ collisions, $d\mathcal{PS} = dy_1 dy_2 dp_\perp^2$ for photon + jet production and $d\mathcal{PS} = dy_1 dy_2 dp_{1\perp} dp_{2\perp}$ for photon + hadron production.

The enhancement of the transverse momentum imbalance (or nuclear broadening) in $h + A$ ($h = p$, γ^*) collisions relative to $h + p$ collisions can be quantified by the difference:

$$\Delta\langle q_\perp^2 \rangle = \langle q_\perp^2 \rangle_{hA} - \langle q_\perp^2 \rangle_{hp}. \tag{3}$$

The broadening $\Delta\langle q_\perp^2 \rangle$ is a result of multiple quark and gluon scattering, and is a direct probe of the nuclear medium properties. We now take into account both initial-state and final-state multiple parton interactions to calculate the nuclear broadening $\Delta\langle q_\perp^2 \rangle$ for photon + jet (photon + hadron) and heavy-quark (heavy-meson) pair production in $p + A$ collisions. In the next section we study di-jet (di-hadron) and heavy-quark (heavy-meson) pair production in $e + A$ collisions.

A. Photon + jet (hadron) production in $p + A$ collisions

1. Photon + jet production

Consider the following back-to-back photon + jet production process (the photons here and throughout the paper are direct photons) in $p + A$ collisions:

$$p(P') + A(P) \to \gamma(p_1) + J(p_2) + X. \tag{4}$$

Here, P', P are the four momentum of the incoming hadron and nucleus (per nucleon) with atomic number A and p_1 and p_2 are the four momentum of the produced final-state photon and jet, respectively. The light-cone components of the final-state particles are given by

$$\begin{aligned} p_1 &= \left[\frac{|\vec{p}_{1\perp}|}{\sqrt{2}} e^{y_1}, \frac{|\vec{p}_{1\perp}|}{\sqrt{2}} e^{-y_1}, \vec{p}_{1\perp} \right], \\ p_2 &= \left[\frac{|\vec{p}_{2\perp}|}{\sqrt{2}} e^{y_2}, \frac{|\vec{p}_{2\perp}|}{\sqrt{2}} e^{-y_2}, \vec{p}_{2\perp} \right], \end{aligned} \tag{5}$$

where $y_{1,2}$ and $\vec{p}_{1,2\perp}$ are the rapidities and transverse momenta, respectively. In leading-order collinear factorized perturbative QCD, the photon and the jet are produced exactly back to back, $\vec{p}_{1\perp} = -\vec{p}_{2\perp}$. It is important to realize that to this order the jet is identical to the leading parton. It is only at next-to-leading order that the QCD structure of the jet starts to play a role in the theoretical description of physics observables. In heavy ion collisions, experimental observables that include jets in the final state are presented after subtraction of the uncorrelated soft hadronic background. Thus, they would be directly comparable to the results presented in this paper. The differential cross section to leading order can be written as [33]

$$\frac{d\sigma}{dy_1 dy_2 dp_\perp^2} = \frac{\pi \alpha_s \alpha_{\rm em}}{s^2} \sum_{a,b} \frac{f_{a/p}(x') f_{b/A}(x)}{x' x} H^U_{ab\to\gamma d}(\hat{s}, \hat{t}, \hat{u}), \tag{6}$$

where $\sum_{a,b}$ runs over all possible parton flavors, $s = (P' + P)^2$ is the center-of-mass energy squared, $f_{a/p}$ and $f_{b/A}$ represent the proton and nuclear parton distribution functions, respectively. At this order in perturbation theory, the parton

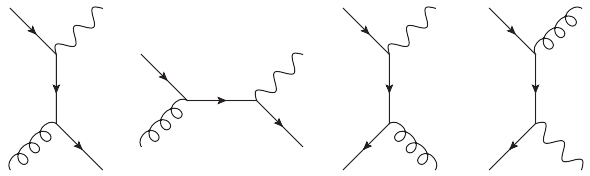

FIG. 1. Leading order Feynman diagrams for photon-jet production.

momentum fractions x' and x are uniquely related to the rapidities and the jet transverse momentum:

$$x' = \frac{p_\perp}{\sqrt{s}}(e^{y_1} + e^{y_2}), \quad x = \frac{p_\perp}{\sqrt{s}}(e^{-y_1} + e^{-y_2}). \tag{7}$$

$H^U_{ab\to cd}(\hat{s}, \hat{t}, \hat{u})$ are the partonic cross sections as a function of the usual partonic Mandelstam variables $\hat{s}, \hat{t}, \hat{u}$. They are calculated from the Feynman diagrams in Fig. 1 and are given by [33,34]

$$H^U_{qg\to\gamma q} = e_q^2 \frac{1}{N_c}\left[-\frac{\hat{s}}{\hat{t}} - \frac{\hat{t}}{\hat{s}}\right], \tag{8}$$

$$H^U_{gq\to\gamma q} = e_q^2 \frac{1}{N_c}\left[-\frac{\hat{s}}{\hat{u}} - \frac{\hat{u}}{\hat{s}}\right], \tag{9}$$

$$H^U_{q\bar{q}\to\gamma g} = e_q^2 \frac{N_c^2 - 1}{N_c^2}\left[\frac{\hat{t}}{\hat{u}} + \frac{\hat{u}}{\hat{t}}\right], \tag{10}$$

where $N_c = 3$ is the number of colors.

In $p + A$ collisions, the energetic incoming parton from the proton can undergo multiple scattering with the soft partons inside the nuclear matter before the hard collisions (initial-state multiple scattering). After the hard collisions, the leading outgoing parton (opposite the photon) will also undergo multiple interactions in the large nucleus (final-state multiple scattering). These interactions lead to an enhancement in the photon + jet transverse momentum imbalance, which can be quantified by $\Delta\langle q_\perp^2\rangle$, as defined in Eq. (3). This nuclear broadening $\Delta\langle q_\perp^2\rangle$ can be calculated in perturbative QCD. A specific method based on double parton scattering has been discussed in detail in Refs. [5,9,12,22]. Our derivation closely follows our previous paper [12]. The leading contribution to the nuclear broadening comes from the double scattering: either initial-state double scattering, as in Figs. 2(a) and 2(c) for the partonic channels $q\bar{q} \to \gamma g$ and $qg \to \gamma q$, respectively; or final-state double scattering, as in Figs. 2(b) and 2(d). We calculate the contributions from these diagrams in the covariant gauge and obtain the following expression for the nuclear broadening of photon + jet production in $p + A$ collisions:

$$\Delta\langle q_\perp^2\rangle = \left(\frac{8\pi^2\alpha_s}{N_c^2 - 1}\right)\frac{\sum_{a,b}\frac{f_{a/p}(x')}{x'x}[T^{(I)}_{b/A}(x)H^I_{ab\to\gamma d}(\hat{s}, \hat{t}, \hat{u}) + T^{(F)}_{b/A}(x)H^F_{ab\to\gamma d}(\hat{s}, \hat{t}, \hat{u})]}{\sum_{a,b}\frac{f_{a/p}(x')f_{b/A}(x)}{x'x}H^U_{ab\to\gamma d}(\hat{s}, \hat{t}, \hat{u})}, \tag{11}$$

where $T^{(I)}_{b/A}(x) = T^{(I)}_{q/A}(x)$ [or $T^{(I)}_{g/A}(x)$] are twist-4 quark-gluon (or gluon-gluon) correlation functions associated with initial-state multiple scattering, with the following operator definitions [5,9,12,22]:

$$T^{(I)}_{q/A}(x) = \int\frac{dy^-}{2\pi}e^{ixp^+y^-}\int\frac{dy_1^-dy_2^-}{2\pi}\theta(y^- - y_1^-)\theta(-y_2^-)\frac{1}{2}\langle p_A|F_\alpha{}^+(y_2^-)\bar{\psi}_q(0)\gamma^+\psi_q(y^-)F^{+\alpha}(y_1^-)|p_A\rangle, \tag{12}$$

$$T^{(I)}_{g/A}(x) = \int\frac{dy^-}{2\pi}e^{ixp^+y^-}\int\frac{dy_1^-dy_2^-}{2\pi}\theta(y^- - y_1^-)\theta(-y_2^-)\frac{1}{xp^+}\langle p_A|F_\alpha{}^+(y_2^-)F^{\sigma+}(0)F^+{}_\sigma(y^-)F^{+\alpha}(y_1^-)|p_A\rangle. \tag{13}$$

On the other hand, $T^{(F)}_{q/A}(x)$ and $T^{(F)}_{g/A}(x)$ are the corresponding twist-4 correlation functions connected with the final-state multiple scattering. They are given by the same expressions in Eqs. (12) and (13), except for the θ functions that are replaced as follows [9,12]:

$$\theta(y^- - y_1^-)\theta(-y_2^-) \to \theta(y_1^- - y^-)\theta(y_2^-). \tag{14}$$

The hard part functions $H^I_{ab\to\gamma d}$ and $H^F_{ab\to\gamma d}$ are associated with initial and final-state multiple scattering, respectively, and are given by

$$H^I_{ab\to\gamma d} = \begin{cases} C_F H^U_{ab\to\gamma d} & \text{a = quark} \\ C_A H^U_{ab\to\gamma d} & \text{a = gluon,} \end{cases} \tag{15}$$

$$H^F_{ab\to\gamma d} = \begin{cases} C_F H^U_{ab\to\gamma d} & \text{d = quark} \\ C_A H^U_{ab\to\gamma d} & \text{d = gluon.} \end{cases} \tag{16}$$

Here, $C_F = (N_c^2 - 1)/2N_c$ and $C_A = N_c$ are the quadratic Casimir in the fundamental and adjoint representations of $SU(3)_c$, respectively. It is also instructive to recall that the strength of the multiple scattering depends on the color representation of the complete scattered parton system [12]. For photon + jet production, since the photon does not carry color, the final-state multiple scattering only depends on the color of the jet parton (whether it is a quark or a gluon), as can be clearly seen in Eq. (16).

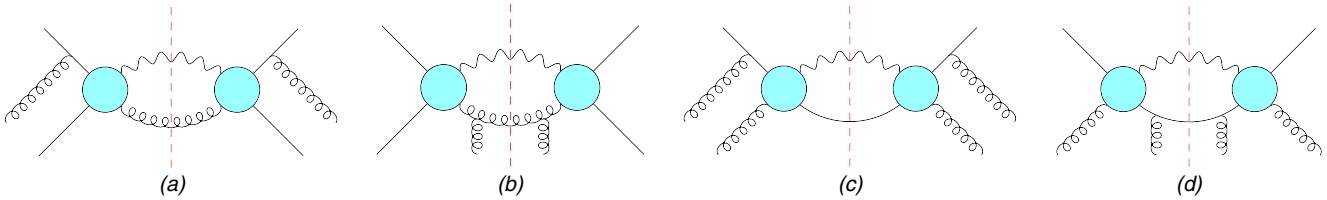

FIG. 2 (color online). Double scattering diagrams for $q\bar{q} \to \gamma g$ (left two) and $qg \to \gamma q$ (right two): (a) and (c) are for initial-state double scattering, while (b) and (d) are for final-state double scattering. The blobs represent the tree-level diagrams as shown in Fig. 1.

2. Photon + hadron production

For the back-to-back photon + hadron production in $p + A$ collisions, $p(P') + A(P) \to \gamma(p_1) + h(p_2) + X$, the leading order differential cross section has the following form:

$$\frac{d\sigma}{dy_1 dy_2 dp_{1\perp} dp_{2\perp}} = \frac{2\pi\alpha_s\alpha_{\rm em}}{s^2}\sum_{abd} D_{h/d}(z)\frac{f_{a/p}(x')f_{b/A}(x)}{x'x}H^U_{ab\to\gamma d}(\hat{s},\hat{t},\hat{u}), \tag{17}$$

where the momentum fractions z, x', and x are given by

$$z = \frac{p_{2\perp}}{p_{1\perp}}, \quad x' = \frac{p_{1\perp}}{\sqrt{s}}(e^{y_1} + e^{y_2}), \quad x = \frac{p_{1\perp}}{\sqrt{s}}(e^{-y_1} + e^{-y_2}). \tag{18}$$

Following our previous paper [12], we can easily generalize the calculation for nuclear broadening $\Delta\langle q_\perp^2\rangle$ in photon + jet to photon + hadron production by including the fragmentation function $D_{h/d}(z)$, and it is given by

$$\Delta\langle q_\perp^2\rangle = \left(\frac{8\pi^2\alpha_s}{N_c^2-1}\right)\frac{\sum_{abd} D_{h/d}(z)\frac{f_{a/p}(x')}{x'x}[T^{(I)}_{b/A}(x)H^I_{ab\to\gamma d}(\hat{s},\hat{t},\hat{u}) + T^{(F)}_{b/A}(x)H^F_{ab\to\gamma d}(\hat{s},\hat{t},\hat{u})]}{\sum_{abd} D_{h/d}(z)\frac{f_{a/p}(x')f_{b/A}(x)}{x'x}H^U_{ab\to\gamma d}(\hat{s},\hat{t},\hat{u})}. \tag{19}$$

B. Heavy-quark (heavy-meson) pair production in $p + A$ collision

1. Heavy-quark pair production

We now study the heavy-quark pair production, $p(P') + A(P) \to Q(p_1) + \bar{Q}(p_2) + X$. At leading order in perturbative QCD, the heavy quark Q and antiquark $\bar{Q}$ are produced back to back through the following partonic channels: $q\bar{q} \to Q\bar{Q}$, $gg \to Q\bar{Q}$. Thus, $\vec{p}_{1\perp} = -\vec{p}_{2\perp}$ and $|\vec{p}_{1\perp}| = |\vec{p}_{2\perp}| \equiv p_\perp$. The differential cross section can be written as

$$\frac{d\sigma}{dy_1 dy_2 dp_\perp^2} = \frac{\pi\alpha_s^2}{s^2}\sum_{a,b}\frac{f_{a/p}(x')f_{b/A}(x)}{x'x}H^U_{ab\to Q\bar{Q}}(\hat{s},\hat{t},\hat{u}), \tag{20}$$

where the parton momentum fractions x' and x are given by

$$x' = \frac{m_\perp}{\sqrt{s}}(e^{y_1} + e^{y_2}), \quad x = \frac{m_\perp}{\sqrt{s}}(e^{-y_1} + e^{-y_2}), \tag{21}$$

with $m_\perp = \sqrt{p_\perp^2 + m_Q^2}$ and m_Q the heavy quark mass. The hard part functions $H^U_{ab\to Qd}$, $H^U_{ab\to\bar{Q}d}$, $H^U_{ab\to Q\bar{Q}}$ for the partonic processes $a(p_a) + b(p_b) \to Q(p_1) + d(p_2)$, $a(p_a) + b(p_b) \to \bar{Q}(p_1) + d(p_2)$, $a(p_a) + b(p_b) \to Q(p_1) + \bar{Q}(p_2)$ relevant to the variable flavor scheme [35] are given in Ref. [36]. In this paper we work in the fixed flavor scheme (three light quarks). Furthermore, if instead of the standard definition of Mandelstam variables one introduces the notation

$$\hat{s} = (p_a + p_b)^2, \qquad \hat{t} = (p_a - p_1)^2 - m_Q^2, \qquad \hat{u} = (p_b - p_1)^2 - m_Q^2, \tag{22}$$

the two relevant hard part functions can be written compactly as [37]

$$H^U_{q\bar{q}\to Q\bar{Q}} = \frac{C_F}{N_c}\left[\frac{\hat{t}^2 + \hat{u}^2 + 2m_Q^2\hat{s}}{\hat{s}^2}\right],$$
$$H^U_{gg\to Q\bar{Q}} = \frac{1}{2N_c}\left[\frac{1}{\hat{t}\,\hat{u}} - \frac{N_c}{C_F}\frac{1}{\hat{s}^2}\right] \times\left[\hat{t}^2 + \hat{u}^2 + 4m_Q^2\hat{s} - \frac{4m_Q^4\hat{s}^2}{\hat{t}\,\hat{u}}\right]. \tag{23}$$

The nuclear enhancement of the transverse momentum imbalance $\Delta\langle q_\perp^2\rangle$ in $p + A$ collisions can be easily calculated and the final result is given by

$$\Delta\langle q_\perp^2\rangle = \left(\frac{8\pi^2\alpha_s}{N_c^2-1}\right)\frac{\sum_{a,b}\frac{f_{a/p}(x')}{x'x}[T^{(I)}_{b/A}(x)H^I_{ab\to Q\bar{Q}}(\hat{s},\hat{t},\hat{u}) + T^{(F)}_{b/A}(x)H^F_{ab\to Q\bar{Q}}(\hat{s},\hat{t},\hat{u})]}{\sum_{a,b}\frac{f_{a/p}(x')f_{b/A}(x)}{x'x}H^U_{ab\to Q\bar{Q}}(\hat{s},\hat{t},\hat{u})}, \tag{24}$$

where the hard functions $H^I_{ab\to Q\bar{Q}}$ and $H^F_{ab\to Q\bar{Q}}$ are again associated with initial-state and final-state multiple scattering and are given by

$$H^I_{q\bar{q}\to Q\bar{Q}} = C_F H^U_{q\bar{q}\to Q\bar{Q}}, \tag{25}$$

$$H^I_{gg\to Q\bar{Q}} = C_A H^U_{gg\to Q\bar{Q}}, \tag{26}$$

$$H^F_{q\bar{q}\to Q\bar{Q}} = C_A H^U_{q\bar{q}\to Q\bar{Q}}, \tag{27}$$

$$H^F_{gg\to Q\bar{Q}} = C_A H^U_{gg\to Q\bar{Q}} - \frac{1}{2(N_c^2-1)}\frac{1}{\hat{t}\,\hat{u}}\left[\hat{t}^2+\hat{u}^2+4m_Q^2\hat{s}-\frac{4m_Q^4\hat{s}^2}{\hat{t}\,\hat{u}}\right]. \tag{28}$$

When the heavy quark mass $m_Q \to 0$, we recover the published results for $H^{I,F}_{q\bar{q}\to q'\bar{q}'}$ and $H^{I,F}_{gg\to q\bar{q}}$ in our previous paper [12].

2. Heavy-meson pair production

One can easily extend the above calculation to heavy-meson pair production, such as back-to-back $D+\bar{D}$, $p(P')+A(P)\to D(p_1)+\bar{D}(p_2)+X$. The differential cross section is given by [36]

$$\frac{d\sigma}{dy_1dy_2dp_{1\perp}dp_{2\perp}} = \frac{2\pi\alpha_s^2}{s^2}\sum_{a,b}\int\frac{dz_1}{z_1}D_{D/Q}(z_1)D_{\bar{D}/\bar{Q}}(z_2)\frac{f_{a/p}(x')f_{b/A}(x)}{x'x}H^U_{ab\to Q\bar{Q}}(\hat{s},\hat{t},\hat{u}), \tag{29}$$

where $D_{D/Q}(z_1)$ and $D_{\bar{D}/\bar{Q}}(z_2)$ are heavy-meson fragmentation functions, $z_2 = z_1 p_{2\perp}/p_{1\perp}$, and

$$x' = \frac{m_\perp}{\sqrt{s}}(e^{y_1}+e^{y_2}), \qquad x = \frac{m_\perp}{\sqrt{s}}(e^{-y_1}+e^{-y_2}), \tag{30}$$

with $m_\perp = \sqrt{(p_{1\perp}/z_1)^2+m_Q^2}$. The nuclear broadening $\Delta\langle q_\perp^2\rangle$ is given by

$$\Delta\langle q_\perp^2\rangle = \left(\frac{8\pi^2\alpha_s}{N_c^2-1}\right)\frac{\sum_{a,b}\int\frac{dz_1}{z_1}D_{D/Q}(z_1)D_{\bar{D}/\bar{Q}}(z_2)\frac{f_{a/p}(x')}{x'x}[T^{(I)}_{b/A}(x)H^I_{ab\to Q\bar{Q}}(\hat{s},\hat{t},\hat{u})+T^{(F)}_{b/A}(x)H^F_{ab\to Q\bar{Q}}(\hat{s},\hat{t},\hat{u})]}{\sum_{a,b}\int\frac{dz_1}{z_1}D_{D/Q}(z_1)D_{\bar{D}/\bar{Q}}(z_2)\frac{f_{a/p}(x')f_{b/A}(x)}{x'x}H^U_{ab\to Q\bar{Q}}(\hat{s},\hat{t},\hat{u})}. \tag{31}$$

Including the di-jet and di-hadron production in our previous paper [12], we have computed the nuclear broadening in the transverse momentum imbalance for all important back-to-back two-particle production channels in $p+A$ collisions. We now study two-particle production in $e+A$ collisions in the next section.

III. NUCLEAR ENHANCEMENT OF THE TRANSVERSE MOMENTUM IMBALANCE IN $e+A$ COLLISIONS

In this section, we use the same approach to calculate the nuclear broadening for di-jet and di-hadron, as well as heavy-quark (heavy-meson) pair production in deep inelastic scattering (DIS) of a lepton on a big nucleus, or γ^*+A collisions. Since the virtual photon does not interact with the soft partons in the nuclear target via the strong force, the nuclear broadening only comes from the final-state multiple scattering.

A. Di-jet (di-hadron) production in DIS

1. Di-jet production

Nuclear enhancement of the di-jet transverse momentum imbalance in photoproduction has been calculated in Ref. [22]. Here we will generalize the result to di-jet production in DIS,

$$\gamma^*(P_{\gamma^*})+A(P)\to J_1(p_1)+J_2(p_2)+X, \tag{32}$$

where the incoming virtual-photon γ^* carries momentum P_{γ^*} with virtuality $P^2_{\gamma^*} = -Q^2$. P is the four momentum of the target nucleus, p_1 and p_2 are the momenta of final-state jets J_1 and J_2, respectively. We will work in the center of mass frame of γ^*+ A, in which the light-cone components of the incoming particles are

$$P_{\gamma^*} = \left[\sqrt{\frac{s}{2}}, -\frac{Q^2}{\sqrt{2s}}, 0_\perp\right], \quad P = \left[0, \frac{s+Q^2}{\sqrt{2s}}, 0_\perp\right]. \tag{33}$$

At leading order, the two jets have opposite transverse momentum but with the same magnitude $p_\perp$, and the differential cross section can be written as

$$\frac{d\sigma}{dy_1 dp_\perp^2} = \frac{\pi\alpha_s\alpha_{\rm em}}{(s+Q^2)^2}\sum_b \frac{1}{1-\frac{p_\perp}{\sqrt{s}}e^{y_1}} \times \frac{f_{b/A}(x)}{x} H^U_{\gamma^* b\to cd}(\hat{s},\hat{t},\hat{u},Q^2), \quad (34)$$

where the momentum fraction x is given by

$$x = x_B + \frac{p_\perp\sqrt{s}}{s+Q^2}\left[e^{-y_1} + \frac{1}{\sqrt{s}/p_\perp - e^{y_1}}\right], \quad (35)$$

with $x_B = Q^2/2P\cdot P_{\gamma^*} = Q^2/(s+Q^2)$. y_1 is the rapidity of the first jet J_1, and the rapidity y_2 of the second jet J_2 is related to y_1 as follows:

$$y_2 = \ln\left(\frac{\sqrt{s}}{p_\perp} - e^{y_1}\right). \quad (36)$$

The hard functions $H^U_{\gamma^* b\to cd}$ are given by

$$H^U_{\gamma^* q\to qg} = e_q^2\frac{N_c^2-1}{N_c}\left[-\frac{\hat{s}}{\hat{t}} - \frac{\hat{t}}{\hat{s}} + \frac{2\hat{u}Q^2}{\hat{s}\,\hat{t}}\right], \quad (37)$$

$$H^U_{\gamma^* g\to q\bar{q}} = e_q^2\left[\frac{\hat{t}}{\hat{u}} + \frac{\hat{u}}{\hat{t}} - \frac{2\hat{s}Q^2}{\hat{t}\,\hat{u}}\right], \quad (38)$$

where $\hat{s}$, $\hat{t}$, and $\hat{u}$ are defined as

$$\hat{s} = (P_{\gamma^*} + xP)^2, \quad \hat{t} = (P_{\gamma^*} - p_1)^2, \quad \hat{u} = (xP - p_1)^2. \quad (39)$$

Since the virtual photon does not interact strongly with the nucleus, the broadening $\Delta\langle q_\perp^2\rangle$ is only sensitive to final-state multiple scattering and is given by

$$\Delta\langle q_\perp^2\rangle = \left(\frac{8\pi^2\alpha_s}{N_c^2-1}\right)\frac{\sum_b \frac{1}{x}T^{(F)}_{b/A}(x)H^F_{\gamma^* b\to cd}(\hat{s},\hat{t},\hat{u},Q^2)}{\sum_b \frac{1}{x}f_{b/A}(x)H^U_{\gamma^* b\to cd}(\hat{s},\hat{t},\hat{u},Q^2)}. \quad (40)$$

The hard function $H^F_{\gamma^* b\to cd}$ can be written as

$$H^F_{\gamma^* b\to cd} = \begin{cases} C_F H^U_{\gamma^* b\to cd} & \text{b = quark} \\ C_A H^U_{\gamma^* b\to cd} & \text{b = gluon.} \end{cases} \quad (41)$$

These expressions suggest that even though $H^F_{\gamma^* b\to cd}$ are the hard functions associated with final-state multiple scattering, the strength of the broadening depends on the color representation of the initial-state parton b: the color factor C_F (or C_A) corresponds to the incoming quark (or gluon). This is not surprising since the rescattering effects are only sensitive to the total color of the final two-parton composite state, which is equal to the color of the initial parton b (as γ^* carries no color). It is easy to show that by setting $Q^2 \to 0$, we recover the result for di-jet photoproduction derived in Ref. [22].

2. Di-hadron production

For back-to-back hadron pair production, $\gamma^*(P_{\gamma^*}) + A(P) \to h_1(p_1) + h_2(p_2) + X$, the differential cross section can be written as

$$\frac{d\sigma}{dy_1 dy_2 dp_{1\perp} dp_{2\perp}} = \frac{2\pi\alpha_s\alpha_{\rm em}}{(s+Q^2)^2}\sum_b D_{h_1/c}(z_1)D_{h_2/d}(z_2) \times \frac{f_{b/A}(x)}{x} H^U_{\gamma^* b\to cd}(\hat{s},\hat{t},\hat{u},Q^2), \quad (42)$$

where the momentum fractions z_1, z_2, and x are given by

$$z_1 = \frac{p_{1\perp}}{\sqrt{s}}(e^{y_1} + e^{y_2}), \qquad z_2 = \frac{p_{2\perp}}{\sqrt{s}}(e^{y_1} + e^{y_2}), \qquad x = x_B + \frac{s}{s+Q^2}\frac{e^{-y_1} + e^{-y_2}}{e^{y_1} + e^{y_2}}. \quad (43)$$

The nuclear broadening $\Delta\langle q_\perp^2\rangle$ has the following form:

$$\Delta\langle q_\perp^2\rangle = \left(\frac{8\pi^2\alpha_s}{N_c^2-1}\right)\frac{\sum_{b,c,d} D_{h_1/c}(z_1)D_{h_2/d}(z_2)\frac{1}{x}T^{(F)}_{b/A}(x)H^F_{\gamma^* b\to cd}(\hat{s},\hat{t},\hat{u},Q^2)}{\sum_{b,c,d} D_{h_1/c}(z_1)D_{h_2/d}(z_2)\frac{1}{x}f_{b/A}(x)H^U_{\gamma^* b\to cd}(\hat{s},\hat{t},\hat{u},Q^2)}. \quad (44)$$

B. Heavy-quark (heavy-meson) pair production in DIS

1. Heavy-quark pair production

We now study the heavy-quark pair production, $\gamma^*(P_{\gamma^*}) + A(P) \to Q(p_1) + \bar{Q}(p_2) + X$. At leading order, there is only one partonic channel that contributes, $\gamma^* + g \to Q + \bar{Q}$ [38]. The differential cross section can be written as

$$\frac{d\sigma}{dy_1 dp_\perp^2} = \frac{\pi\alpha_s\alpha_{\rm em}}{(s+Q^2)^2}\frac{1}{1-\frac{m_\perp}{\sqrt{s}}e^{y_1}} \times \frac{f_{g/A}(x)}{x} H^U_{\gamma^* g\to Q\bar{Q}}(\hat{s},\hat{t},\hat{u},Q^2,m_Q^2), \quad (45)$$

where y_1 is the rapidity of the heavy quark Q, while the heavy antiquark $\bar{Q}$ has rapidity $y_2 = \ln(\sqrt{s}/m_\perp - e^{y_1})$. The momentum fraction x is given by

$$x = x_B + \frac{m_\perp \sqrt{s}}{s + Q^2}\left[e^{-y_1} + \frac{1}{\sqrt{s}/m_\perp - e^{y_1}}\right], \quad (46)$$

with the transverse mass $m_\perp = \sqrt{p_\perp^2 + m_Q^2}$. The hard part function $H^U_{\gamma^* g \to Q\bar{Q}}$ has the following form:

$$H^U_{\gamma^* g \to Q\bar{Q}} = e_q^2\left[\frac{\hat{t}}{\hat{u}} + \frac{\hat{u}}{\hat{t}} - \frac{2\hat{s}Q^2}{\hat{t}\,\hat{u}} - \frac{2m_Q^2}{\hat{t}\,\hat{u}} \times \left(\frac{2m_Q^2(\hat{t}+\hat{u})^2}{\hat{t}\,\hat{u}} - Q^2\left(\frac{\hat{t}}{\hat{u}} + \frac{\hat{u}}{\hat{t}}\right) + 2(\hat{t}+\hat{u})\right)\right]. \quad (47)$$

Once again $\hat{s}$, $\hat{t}$, and $\hat{u}$ differ slightly from the standard Mandelstam variables and are given by

$$\hat{s} = (P_{\gamma^*} + xP)^2, \qquad \hat{t} = (P_{\gamma^*} - p_1)^2 - m_Q^2, \qquad \hat{u} = (xP - p_1)^2 - m_Q^2. \quad (48)$$

The nuclear enhancement of the transverse momentum imbalance can be written as

$$\Delta\langle q_\perp^2\rangle = \left(\frac{8\pi^2\alpha_s}{N_c^2 - 1}\right)\frac{\frac{T^{(F)}_{g/A}(x)}{x} H^F_{\gamma^* g \to Q\bar{Q}}(\hat{s}, \hat{t}, \hat{u}, Q^2, m_Q^2)}{\frac{f_{g/A}(x)}{x} H^U_{\gamma^* g \to Q\bar{Q}}(\hat{s}, \hat{t}, \hat{u}, Q^2, m_Q^2)}, \quad (49)$$

where $H^F_{\gamma^* g \to Q\bar{Q}} = C_A H^U_{\gamma^* g \to Q\bar{Q}}$ with C_A reflective of the color representation of the $Q\bar{Q}$ system.

2. Heavy-meson pair production

One can also easily generalize the above calculation to heavy-meson pair production, such as back-to-back $D + \bar{D}$ production, $\gamma^*(P_{\gamma^*}) + A(P) \to D(p_1) + \bar{D}(p_2) + X$. The differential cross section is given by

$$\frac{d\sigma}{dy_1 dy_2 dp_{1\perp} dp_{2\perp}} = \frac{2\pi\alpha_s\alpha_{\rm em}}{(s+Q^2)^2} D_{D/Q}(z_1) D_{\bar{D}/\bar{Q}}(z_2) \times \frac{f_{g/A}(x)}{x} H^U_{\gamma^* g \to Q\bar{Q}}(\hat{s}, \hat{t}, \hat{u}, Q^2), \quad (50)$$

where the momentum fractions z_1 and z_2 in heavy-meson fragmentation functions are given by

$$z_1 = \frac{p_{1\perp}}{r\sqrt{s}}(e^{y_1} + e^{y_2}), \quad z_2 = \frac{p_{2\perp}}{r\sqrt{s}}(e^{y_1} + e^{y_2}). \quad (51)$$

Here the parameter r depends on the heavy quark mass m_Q:

$$r = \sqrt{1 - \left[\frac{m_Q}{\sqrt{s}}(e^{y_1} + e^{y_2})\right]^2}. \quad (52)$$

The nuclear broadening for this final state is given by

$$\Delta\langle q_\perp^2\rangle = \left(\frac{8\pi^2\alpha_s}{N_c^2 - 1}\right) \times \frac{D_{D/Q}(z_1) D_{\bar{D}/\bar{Q}}(z_2) \frac{T^{(F)}_{g/A}(x)}{x} H^F_{\gamma^* g \to Q\bar{Q}}(\hat{s}, \hat{t}, \hat{u}, Q^2)}{D_{D/Q}(z_1) D_{\bar{D}/\bar{Q}}(z_2) \frac{f_{g/A}(x)}{x} H^U_{\gamma^* g \to Q\bar{Q}}(\hat{s}, \hat{t}, \hat{u}, Q^2)}. \quad (53)$$

We have now completed all evaluations of the nuclear enhancement of the transverse momentum imbalance in back-to-back two-particle production in both $p + A$ and $e + A$ collisions. We will use these expressions to present predictions for $\Delta\langle q_\perp^2\rangle$ relevant to future experimental measurements in the next section.

IV. NUMERICAL RESULTS

In this section we present phenomenological applications of our results. Specifically, we give theoretical predictions for the nuclear broadening (or enhancement of the transverse momentum imbalance) for back-to-back particle production in $d + Au$ collisions at RHIC, for the forthcoming $p + Pb$ collisions at LHC, and for the $e + A$ collisions at the planned EIC and LHeC. The only new unknown ingredient in our calculation is the twist-4 quark-gluon and gluon-gluon correlation functions. Following [12,30,31], we parametrize them as follows:

$$\frac{4\pi^2\alpha_s}{N_c} T^{(I)}_{q,g/A}(x) = \frac{4\pi^2\alpha_s}{N_c} T^{(F)}_{q,g/A}(x) = \xi^2(A^{1/3} - 1) f_{q,g/A}(x), \quad (54)$$

where $f_{q,g/A}(x)$ is the standard leading-twist parton distribution function for quarks or gluons, respectively. In Eq. (54) $\xi^2 = 0.12$ GeV^2 represents a characteristic scale of parton multiple scattering and was extracted from deep inelastic scattering data [30]. The definition in Eq. (54) is such that $\xi^2(A^{1/3} - 1)$ can be thought of as a dynamical quark mass generated in the background soft gluon field of the nucleus in minimum-bias reactions [39]. Our implementation has also been successful in describing the nuclear suppression of single inclusive hadron production [31,36] and the di-hadron transverse momentum imbalance and correlations in $d + Au$ collisions at forward rapidities at RHIC $\sqrt{s} = 200$ GeV [12].

As demonstrated in Ref. [30], by approximately decomposing a nuclear state into a product of nucleon states the parameter ξ^2 can be expressed in terms of an averaged gluon field strength squared $\langle F^{+\alpha} F^+{}_\alpha\rangle \sim \lim_{x\to 0} x f_{g/A}(x)$, the soft-gluon number density. In this picture, ξ^2 represents the strength of the multiple scattering, thus proportional to the number of the soft gluons in the nuclear medium. While at tree level ξ^2 is a fixed number, higher order corrections may provide energy dependence to this parameter (for example, at LHC energies ξ^2 can be larger in comparison to the one used at RHIC energies). We study this possibility

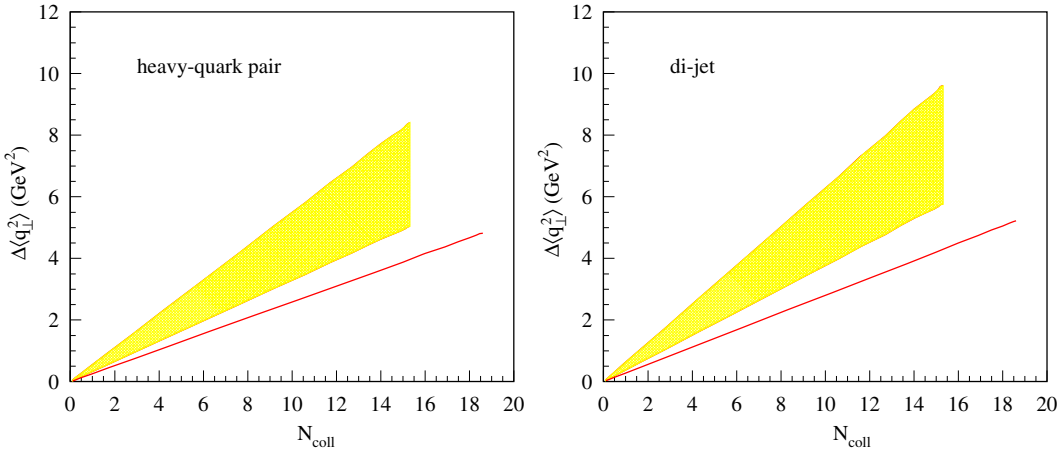

FIG. 3 (color online). Nuclear broadening $\Delta\langle q_\perp^2\rangle$ for back-to-back heavy-quark pairs (left) and di-jets (right) in $p + A$ collisions as a function of binary collision number $N_{\rm coll}$. We choose rapidities $y_1 = y_2 = 2$ for the $\sqrt{s} = 5$ TeV LHC p + Pb collisions and $y_1 = y_2 = 1$ for the $\sqrt{s} = 200$ GeV RHIC d + Au collisions. For the LHC, the jet transverse momentum is integrated over 30 GeV $< p_\perp <$ 40 GeV, while for RHIC the jet transverse momentum is integrated over 15 GeV $< p_\perp <$ 25 GeV. The yellow band is for LHC kinematics, with the band representing a variation of ξ^2 parameter from 0.12 to 0.20 GeV^2. The red solid curve is for RHIC kinematics with $\xi^2 = 0.12$ GeV^2.

phenomenologically by presenting results for a range of ξ^2 from 0.12 to 0.20 GeV^2 at the LHC (yellow band). For the upper limit we take guidance from the growth of the inelastic scattering cross section, from $\sigma_{\rm in}^{\rm RHIC} = 42$ mb at $\sqrt{s} = 200$ GeV to $\sigma_{\rm in}^{\rm LHC} = 70$ mb at $\sqrt{s} = 5$ TeV [40,41]. The energy dependence of ξ^2 (if any) can be tested and further constrained once experimental data at different center-of-mass energies become available.[1] To estimate the transverse momentum broadening for the new channels derived in the last two sections, we use the CTEQ6L for nucleon parton distribution functions [44], and EPS08 parametrization for nuclear parton distribution functions [45]. Since the nuclear broadening $\Delta\langle q_\perp^2\rangle$ is a ratio of cross sections as in Eq. (3), it has very weak dependence on the parametrization for nuclear parton distribution functions.

In Fig. 3 (left) we plot the nuclear enhancement of the transverse momentum imbalance $\Delta\langle q_\perp^2\rangle$ for a back-to-back heavy-quark pair in $p + A$ collisions as a function of the binary collision number $N_{\rm coll}$. To take into account the centrality dependence, we have replaced $(A^{1/3} - 1)$ by $(A^{1/3} - 1)\langle N_{\rm coll}(b)\rangle/\langle N_{\rm coll}(b_{\rm min.bias})\rangle$. We choose the rapidities of both the heavy quark and the antiquark to be $y_1 = y_2 = 2$, and integrate over the transverse momentum 30 GeV $< p_\perp <$ 40 GeV for LHC $p + Pb$ run at $\sqrt{s} =$ 5 TeV, and $y_1 = y_2 = 1$ and 15 GeV $< p_\perp <$ 25 GeV for RHIC $d + Au$ run at $\sqrt{s} = 200$ GeV. The yellow band is for LHC kinematics, with the band representing a variation of the ξ^2 parameter from 0.12 to 0.20 GeV^2 as we discussed above. The red solid curve is for RHIC kinematics with $\xi^2 = 0.12$ GeV^2. For comparison, we also plot in Fig. 3 (right) the nuclear broadening for di-jet production using the same kinematics. We find that the nuclear broadening $\Delta\langle q_\perp^2\rangle$ is slightly stronger for di-jet production when compared to heavy-quark pair production. This is because there are more partonic channels that contribute to the di-jet. In particular, the $gg \to gg$ channel is the most important and generates the largest broadening [12]. However, this channel does not contribute to heavy-quark pair production. Since the $gg \to gg$ channel becomes more important at larger center-of-mass energies, we expect the difference in $\Delta\langle q_\perp^2\rangle$ between heavy-quark pair production and di-jet production to become slightly larger in going from RHIC to the LHC. This can be seen clearly in our predictions in Fig. 3.

In Fig. 4 (left) we plot $\Delta\langle q_\perp^2\rangle$ for the photon + jet final state in $p + A$ collision as a function of $N_{\rm coll}$. Compared to the heavy quark or di-jet production in Fig. 3, the nuclear broadening is much smaller. This is because there is much stronger final-state multiple scattering in di-jet or heavy quark pair production: both outgoing partons interact with the cold nuclear matter. The difference in $\Delta\langle q_\perp^2\rangle$ between photon + jet and di-jet (or heavy-quark pair) production is a direct prediction of our approach. A comparative experimental study facilitated by future experimental measurements will be a very useful test of our formalism. In Fig. 4 (right), we also provide a plot for back-to-back photon + hadron production in $p + A$ collisions as a function of $N_{\rm coll}$. We find that the magnitude of the nuclear enhancement in the transverse momentum imbalance is very similar between photon + jet and photon + hadron production. This is expected since the nuclear broadening as defined in Eqs. (2) and (3) is a ratio of cross sections and should not be affected much by the fragmentation function (the hadronization process).

[1]Recent comparison of theoretical predictions for the cross section modification in $p + Pb$ reactions [42] to new ALICE preliminary data [43] does not favor a growth of ξ^2.

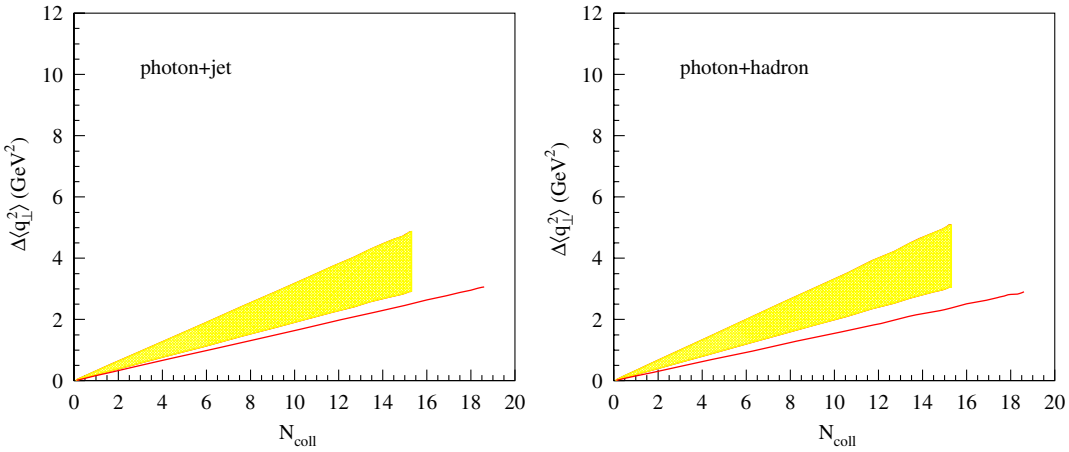

FIG. 4 (color online). Left panel: nuclear broadening $\Delta\langle q_\perp^2\rangle$ for back-to-back photon + jet production in $p + A$ collisions as a function of the binary collision number $N_{\rm coll}$. We choose rapidities $y_1 = y_2 = 2$ for the $\sqrt{s} = 5$ TeV LHC $p + Pb$ collisions and $y_1 = y_2 = 1$ for the $\sqrt{s} = 200$ GeV RHIC $d + Au$ collisions. For the LHC, the jet transverse momentum is integrated over 30 GeV $< p_\perp <$ 40 GeV, while for RHIC the jet transverse momentum is integrated over 15 GeV $< p_\perp <$ 25 GeV. Right panel: same as left plot, but now for back-to-back photon+hadron production. For LHC kinematics, we integrate over $10 < p_{\gamma\perp} < 20$ GeV and $5 < p_{h\perp} < 10$ GeV. For RHIC kinematics, we integrate over $5 < p_{\gamma\perp} < 15$ GeV and $5 < p_{h\perp} < 10$ GeV. The yellow band is for LHC kinematics, with the band representing a variation of ξ^2 parameter from 0.12 to 0.20 GeV^2. The red solid curve is for RHIC kinematics with $\xi^2 = 0.12$ GeV^2.

Nuclear-enhanced transverse momentum imbalance in di-jet and heavy-quark pair production in DIS can provide a clean measurement of final-state rescattering effect. In Fig. 5 we plot $\Delta\langle q_\perp^2\rangle$ for both di-jet and heavy-quark pair production in $\gamma^* + A$ collisions as a function of the atomic number A. In the left panel we present predictions for the relevant kinematics region for the planned future EIC. We choose the $\gamma^* + A$ center-of-mass energy $\sqrt{s} = 100$ GeV and the photon virtuality $Q^2 = 16$ GeV^2. Note that the γ^*-A center-of-mass energy corresponds to the standard DIS kinematic variable W: $s = (P_{\gamma^*} + P)^2 = W^2$. We choose the jet rapidity to be $y_1 = 2$ and integrate the jet transverse momentum over 5 GeV $< p_\perp <$ 10 GeV. In the right panel we present predictions for the relevant kinematics region for the planned future LHeC. We choose the $\gamma^* + A$ center-of-mass energy $\sqrt{s} = 800$ GeV and the photon virtuality $Q^2 = 25$ GeV^2, and integrate the jet transverse momentum over 10 GeV $< p_\perp <$ 20 GeV.

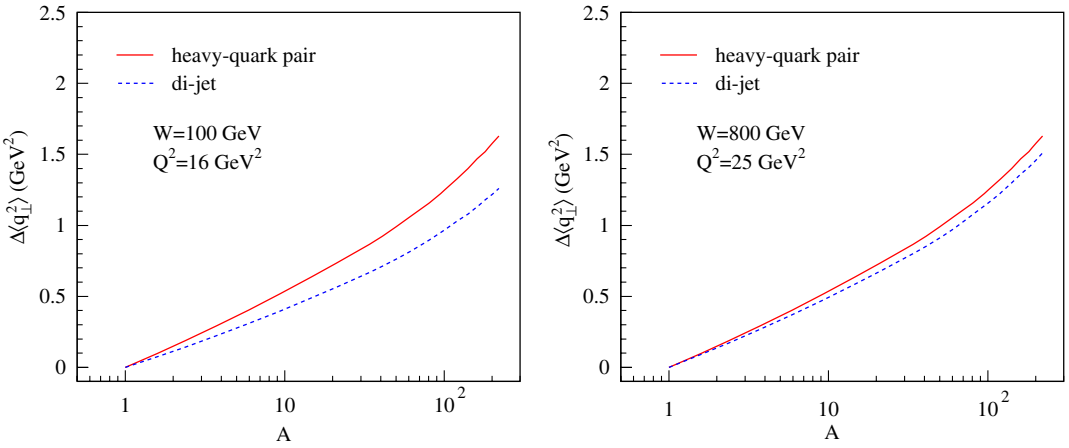

FIG. 5 (color online). Transverse momentum imbalance increase $\Delta\langle q_\perp^2\rangle$ in $\gamma^* + A$ collision as a function of the atomic number A at γ^*-A center-of-mass energy. Left panel: $\sqrt{s} = 100$ GeV and photon virtuality $Q^2 = 16$ GeV^2 for typical EIC kinematics. We choose the jet rapidity $y_1 = 2$ and have integrated the jet transverse momentum over 5 GeV $< p_\perp <$ 10 GeV. Right panel: $\sqrt{s} = 800$ GeV and photon virtuality $Q^2 = 25$ GeV^2 for typical LHeC kinematics [46]. We choose the jet rapidity $y_1 = 2$ and have integrated the jet transverse momentum over 10 GeV $< p_\perp <$ 20 GeV. Note that the γ^*-A center of mass energy corresponds to the standard DIS kinematic variable W: $s = (P_{\gamma^*} + P)^2 = W^2$. The solid curve is for heavy-quark pair production, while the dashed curve is for di-jet production.

Our numerical results show that contrary to the case in $p + A$ collisions, the growth of the transverse momentum imbalance for heavy-quark pair production is larger than that for di-jet production because of the different color factors of the rescattering final state. In the heavy-quark case, only one process is present at leading order and the initial-state parton is a gluon. This gives rise to a color factor C_A. On the other hand, there are two processes that contribute to the di-jet transverse momentum imbalance and they give rise to a combination of color factors: C_F and C_A. Consequently, the nuclear broadening is smaller than the one observed in heavy-quark pair production.

V. SUMMARY

Within a high-twist approach to parton interactions in cold nuclear matter we studied the nuclear enhancement of the transverse momentum imbalance for photon + jet and photon + hadron production in $p + A$ collisions, di-jet and di-hadron production in $e + A$ collisions, and heavy-quark (heavy-meson) pair production in both $p + A$ and $e + A$ collisions. By taking into account both initial-state and final-state multiple scattering, we derived results to lowest order in perturbative QCD for the increase in the transverse momentum imbalance of two particle-production for these channels. We presented numerical predictions for the kinematic regions relevant to $d + Au$ collision at RHIC, $p + Pb$ collisions at LHC, and $e + A$ collisions at a future EIC and LHeC. We found that the nuclear broadening in photon + jet (photon + hadron) production is much smaller than the one in di-jet (or heavy-quark pair) production, due to weaker final-state multiple scattering. It is also interesting to notice that in $p + A$ collisions the di-jet accumulates more nuclear-induced transverse momentum imbalance than the heavy-quark pair production, while in $e + A$ collisions it is the other way around. The difference in the nuclear broadening among the various channels is a direct prediction of our approach. We emphasize that a comparative study of the transverse momentum imbalance of back-to-back particle production, facilitated by future experimental measurements, will be a valuable probe for the multiple scattering effect in cold nuclear matter and a test of our theoretical formalism.

ACKNOWLEDGMENTS

This research is supported by the U.S. Department of Energy, Office of Science, under Contract No. DE-AC52-06NA25396, and in part by the LDRD program at LANL, NSFC of China under Project No. 10825523.

[1] See, for example, M. Gyulassy, I. Vitev, X.-N. Wang, and B.-W. Zhang, arXiv:nucl-th/0302077; B. Muller, J. Schukraft, and B. Wyslouch, arXiv:1202.3233 [Annu. Rev. Nucl. Part. Sci. (to be published)].
[2] See, for example, D. Boer, M. Diehl, R. Milner, R. Venugopalan, W. Vogelsang, D. Kaplan, H. Montgomery, S. Vigdor *et al.*, arXiv:1108.1713.
[3] C. A. Salgado *et al.*, J. Phys. G **39**, 015010 (2012); S. Abreu, V. Akkelin, J. Alam, J. L. Albacete *et al.*, J. Phys. G **35**, 054001 (2008).
[4] Z.-B. Kang and F. Yuan, Phys. Rev. D **84**, 034019 (2011); Z.-B. Kang, S. Mantry, and J.-W. Qiu, arXiv:1204.5469.
[5] X. f. Guo, Phys. Rev. D **58**, 114033 (1998).
[6] A. Airapetian *et al.* (HERMES Collaboration), Phys. Lett. B **684**, 114 (2010).
[7] S. Domdey, D. Grunewald, B. Z. Kopeliovich, and H. J. Pirner, Nucl. Phys. **A825**, 200 (2009).
[8] R. J. Fries, Phys. Rev. D **68**, 074013 (2003).
[9] Z.-B. Kang and J.-W. Qiu, Phys. Rev. D **77**, 114027 (2008).
[10] A. Accardi, arXiv:hep-ph/0212148.
[11] I. Vitev, Phys. Lett. B **562**, 36 (2003).
[12] Z. B. Kang, I. Vitev, and H. Xing, Phys. Rev. D **85**, 054024 (2012).
[13] J. Dolejsi, J. Hufner, and B. Z. Kopeliovich, Phys. Lett. B **312**, 235 (1993).
[14] M. B. Johnson, B. Z. Kopeliovich, and A. V. Tarasov, Phys. Rev. C **63**, 035203 (2001).
[15] R. Baier, Y. L. Dokshitzer, A. H. Mueller, S. Peigne, and D. Schiff, Nucl. Phys. **B484**, 265 (1997).
[16] M. Gyulassy, P. Levai, and I. Vitev, Phys. Rev. D **66**, 014005 (2002).
[17] A. Dumitru and J. Jalilian-Marian, Phys. Lett. B **547**, 15 (2002).
[18] J. L. Albacete and C. Marquet, Phys. Rev. Lett. **105**, 162301 (2010); A. Stasto, B.-W. Xiao, and F. Yuan, Phys. Lett. B **716**, 430 (2012).
[19] A. Idilbi and A. Majumder, Phys. Rev. D **80**, 054022 (2009).
[20] G. Ovanesyan and I. Vitev, J. High Energy Phys. 06 (2011) 080.
[21] F. D'Eramo, H. Liu, and K. Rajagopal, Phys. Rev. D **84**, 065015 (2011).
[22] M. Luo, J.-W. Qiu, and G. F. Sterman, Phys. Rev. D **49**, 4493 (1994).
[23] J. Raufeisen, Phys. Lett. B **557**, 184 (2003).
[24] J.-w. Qiu and G. F. Sterman, Nucl. Phys. **B353**, 105 (1991); J.-w. Qiu and G. F. Sterman, Nucl. Phys. **B353**, 137 (1991).
[25] M. Luo, J.-w. Qiu, and G. F. Sterman, Phys. Lett. B **279**, 377 (1992).
[26] J.-w. Qiu and G. F. Sterman, Int. J. Mod. Phys. E **12**, 149 (2003).
[27] H. Xing, Y. Guo, E. Wang, and X. N. Wang, Nucl. Phys. **A879**, 77 (2012).
[28] X. f. Guo and X. N. Wang, Phys. Rev. Lett. **85**, 3591 (2000).

[29] X. N. Wang and X. f. Guo, Nucl. Phys. **A696**, 788 (2001).
[30] J.-w. Qiu and I. Vitev, Phys. Rev. Lett. **93**, 262301 (2004).
[31] J.-w. Qiu and I. Vitev, Phys. Lett. B **632**, 507 (2006).
[32] Z.-B. Kang and J.-W. Qiu, J. Phys. G **34**, S607 (2007).
[33] J. F. Owens, Rev. Mod. Phys. **59**, 465 (1987).
[34] Z.-B. Kang and I. Vitev, Phys. Rev. D **84**, 014034 (2011).
[35] F. I. Olness, R. J. Scalise, and W.-K. Tung, Phys. Rev. D **59**, 014506 (1998).
[36] I. Vitev, J. T. Goldman, M. B. Johnson, and J. W. Qiu, Phys. Rev. D **74**, 054010 (2006).
[37] Z.-B. Kang, J.-W. Qiu, W. Vogelsang, and F. Yuan, Phys. Rev. D **78**, 114013 (2008).
[38] Z.-B. Kang and J.-W. Qiu, Phys. Rev. D **78**, 034005 (2008).
[39] J.-W. Qiu and I. Vitev, Phys. Lett. B **587**, 52 (2004).
[40] M. L. Miller, K. Reygers, S. J. Sanders, and P. Steinberg, Annu. Rev. Nucl. Part. Sci. **57**, 205 (2007).
[41] D. G. d'Enterria, arXiv:nucl-ex/0302016; see also https://twiki.cern.ch/twiki/bin/view/Main/LHCGlauberBaseline.
[42] Z.-B. Kang, I. Vitev, and H. Xing, arXiv:1209.6030.
[43] B. Abelev *et al.* (ALICE Collaboration), arXiv:1210.4520.
[44] J. Pumplin, D. R. Stump, J. Huston, H. L. Lai, P. M. Nadolsky, and W. K. Tung, J. High Energy Phys. 07 (2002) 012.
[45] K. J. Eskola, H. Paukkunen, and C. A. Salgado, J. High Energy Phys. 07 (2008) 102.
[46] J. L. A. Fernandez *et al.* (LHeC Study Group Collaboration), J. Phys. G **39**, 075001 (2012).